Active transverse mode control and optimisation of an all-solid-state laser using an intracavity adaptive-optic mirror

Active transverse mode control and optimisation of an all-solid-state laser using an intracavity adaptive-optic mirror

Walter Lubeigt, Gareth Valentine, John Girkin, Erwin Bente, David Burns

Institute of Photonics, University of Strathclyde, 106 Rottenrow, Glasgow G4 0NW, United Kingdom
walter.lubeigt@strath.ac.uk

Abstract: A 37 element adaptive optic mirror has been used intracavity to control the oscillation mode profile of a diode-laser pumped Nd:YVO_4 laser. Mode and power optimisation are demonstrated by closed loop automatic optimisation of the deformable mirror.

OCIS codes: (140.3580) Lasers, solid-state; (140.6810) Thermal effects; (999.9999) Adaptive optics, lasers

References and Links

1. J.M. Eggleston, T.J. Kane, K. Kuhn, J. Unternahrer, and R.L. Byer, "The slab geometry laser. I. Theory," IEEE J. Quantum Electron. **QE-20**, 289-301, (1984).
2. W.Koechner, *Solid-State Laser Engineering*, 5th edition (Springer Series in Optical Sciences, 1999).
3. D. Burns, G.J. Valentine, W. Lubeigt, E. Bente, A.I. Ferguson, "Development of High Average Power Picosecond Laser Systems," Proc SPIE **4629**, 4629-18, (2002).
4. D.A. Rockwell, "A review of phase-conjugate solid-state lasers," IEEE J. Quantum Electron. **24**, 1124-1140, (1988).
5. S. Makki, J. Leger, "Solid-state laser resonators with diffractive optic thermal aberration correction," IEEE J. Quantum Electron. **35**, 1075-1085, (1999).
6. R.Tyson, *Principles of Adaptive Optics*, 2nd edition, (Academic Press, 1998).
7. Flexible Optical B.V., PO Box 581, 2600 AN, Delft, the Netherlands, www.okotech.com
8. G. Vdovin G, P.M. Sarro, S. Middelhoek, "Technology and applications of micro-machined adaptive mirrors," J. Micromech. Microeng. **9**, R8-R19 (1999).
9. G. Vdovin, V. Kiyko, "Intracavity control of a 200-W continuous-wave Nd:YAG laser by a micro-machined deformable mirror," Opt. Lett. **26**, 798-800 (2001).
10. K.F. Man, *Genetic Algorithms: concepts and designs*, (Springer Series, 1999).
11. S. Kirkpatrick, C.D. Gelatt, Jr., and M.P. Vecchi, "Optimization by simulated annealing," Science **220** (4598), 671-680 (1983).

1. Introduction

Thermal induced distortion in the gain element is the main obstacle to be overcome in the scaling of solid-state lasers to very high output powers [1]. The problems of obtaining good single transverse mode oscillation and stability from high average power lasers are related to the heat load induced by the high pump powers deposited into the gain medium [2]. The performance is then degraded due to thermally induced birefringence and lensing in the gain material. Careful selection of the host laser material can greatly reduce thermal birefringence and leads to higher output powers but inevitably the heat load and the associated resultant thermal lens will dominate the laser performance. The effects of the spherical contribution of the thermal lens can be effectively reduced by good cavity design [3], however, the non-spherical component cannot be compensated in the same manner, and so eventually leads to reduced efficiency and multi-mode oscillation as the heat load increases. Phase conjugating mirrors applied to master-oscillator power amplifier (MOPA) configurations [4] and diffractive optic elements [5] have been employed to minimise thermal distortions in high power lasers; however practical applications of these devices are limited in terms of their complexity, the loss introduced, and the inability to operate over a wide power range.

#1298 - $15.00 US Received May 30, 2002; Revised June 24, 2002

In this paper we investigate the potential for intracavity aberration control using an electronically addressable deformable membrane mirror. The particular problem addressed is that of transverse mode control using a computer controlled feedback scheme to enable automatic, or self-optimisation of the laser. Deformable membrane mirrors have recently been developed for use in astronomical and medical imaging [6]. The electronic nature of the control of the mirror curvature with a suitable mode-quality detector, gives unique possibilities for real-time alignment and optimisation when accompanied by suitable computer controlled feedback.

2. Micro-machined deformable mirror

The 15mm diameter, OKOTECH [7] deformable membrane mirror, as shown in figure 1, comprised 37 hexagonal actuators arranged in a hexagonal pattern [8]. An additional 12 layer dielectric mirror coating was deposited onto the aluminium coated silicon nitride membrane to provide high reflectivity and low absorption at 1064nm. The maximum specified surface deflection range was 4μm at 290V, however, in these experiments the maximum actuator voltage activated was intentionally limited to 200V. Similar mirrors have been demonstrated at optical power densities of 2.6kW/cm^2 (intracavity) and 11kW/cm^2 (extracavity) without damage [9].

The actuators could be individually addressed via a personal computer using a homemade software package with a graphic user interface using LabWindows/CVI (National Instruments Ltd). The output from the PC was from two 20 channel 8-bit DAC converters. Each channel was then amplified using a multi-channel voltage amplifier before being applied to the individual electrostatic transducers of the Adaptive-Optic mirror. It is worth noting that the electrostatic transducers can only 'pull' the membrane surface from its zero-bias state. The mirror therefore may require a pre-bias to meet the demands of some applications. The AO mirror was held in a protective mount with a 1064nm anti reflection coated front window in order to minimise any vibration, draught or deposition of dust on the membrane.

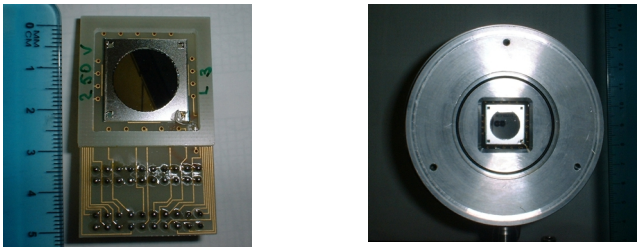

Figure 1. The deformable membrane mirror (LHS) and, the mirror housing used in these experiments (RHS). Note: that an anti-reflection coated window is used to environmentally shield the fragile mirror surface and reduce the effects of air currents.

3. Experimental laser cavity set-up

To investigate the use of an intracavity deformable mirror to optimise the modal performance of an all-solid-state laser, the Nd:YVO_4 resonator of figure 2a was configured. The 150mm focal length lens ensured a large (~7mm diameter) spot on the adaptive mirror such that the beam covered as many actuators as possible. In this way the resolution of the beam/mirror interaction could be enhanced allowing a greater degree of optimisation to be performed. The resonator exhibited a stability region that was suitably covered by the range of curvatures available with the adaptive mirror (see fig. 2b).

The gain medium was a 2mm thick HR-AR coated Nd:YVO_4 crystal and was pumped using a fibre coupled diode emitting at 808nm. The pump power could be adjusted from 0 to 10W. A 98% reflective mirror was initially used as the output coupler (M1) giving 120mW output power when optimized with the AO mirror at 6W pump power. It should be noted that the laser was configured specifically to demonstrate automated mode control and not to

#1298 - $15.00 US Received May 30, 2002; Revised June 24, 2002

optimise the power transfer efficiency; hence no attempt was made to maximise the overlap between the pump mode and the laser mode.

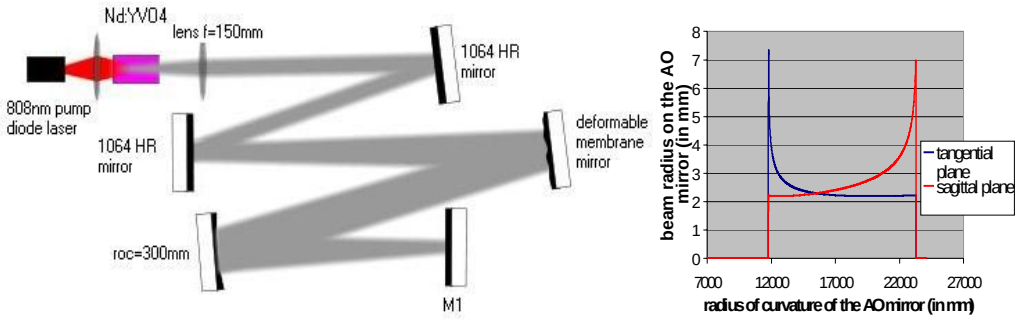

2a 2b

Figure 2. (a) Schematic of the Nd:YVO_4 laser cavity arrangement and diagnostics used to perform active transverse mode control. (b) Beam radius on the AO mirror as a function of the radius of curvature of the AO mirror.

4. Optimisation methods

4.1 Physical aperture

A manual optimisation routine was sufficient to demonstrate the effectiveness of the AO mirror for laser mode control, however, the optimisation procedure was somewhat time consuming and subjective. So in order to demonstrate automatic control of the laser, two arrangements were investigated. In the first, the output from the laser was spatially filtered by being apertured through a 100μm pinhole onto a silicon photodiode. The control program was then configured to maximise the power detected by the photodiode; in this way the feedback loop substantially favoured oscillation on a TEM_{00} mode. A schematic of the automatic closed loop optimisation scheme is depicted in figure 3.

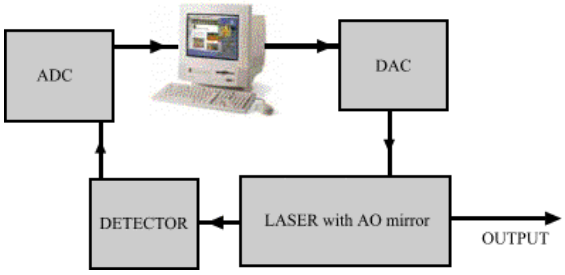

Figure 3. Schematic of the closed loop feedback network used for the self-optimising laser.

4.2 Software aperture

In a further development, the control software utilised an input from a Pulnix Progressive Scan and frame grabber CCD camera such that a user-selectable ‘software aperture’ can be employed. The modal output from the laser was assessed by the integrated pixel intensity within the selected ‘software aperture’ of the CCD camera image. The dimensions, the location and averaging within the aperture could all be set for optimal performance. The interface for the automatic optimisation software is shown in figure 4.

#1298 - $15.00 US
Received May 30, 2002; Revised June 24, 2002

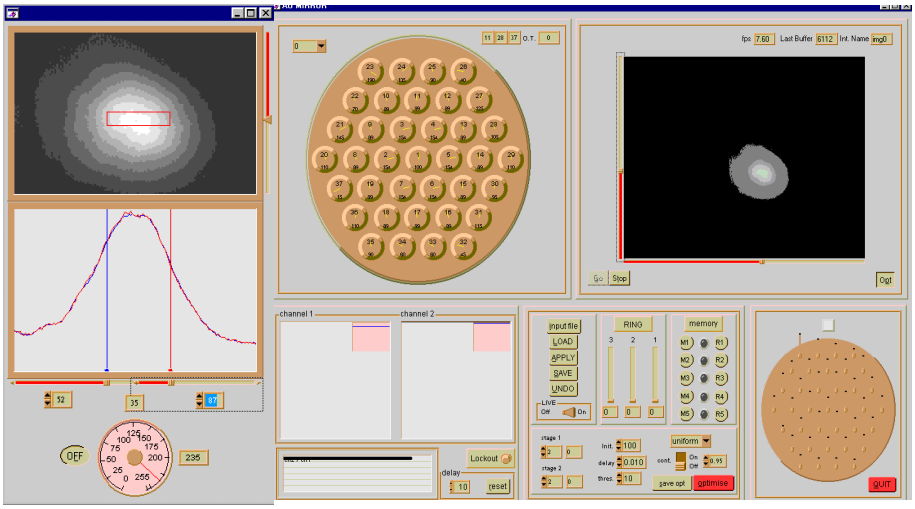

Figure 4. Graphic User Interface for manual and automatic laser optimisation. The panel on the left displays a zoomed area of the larger camera image on the main screen, and enables the control signal for the optimisation loop to be configured.

4.3 Optimisation algorithm

The optimisation scheme described here has been demonstrated to work well for this simple laser arrangement. The optimisation procedure used was based on a modification of a two stage 'hill-climbing' algorithm. [A more comprehensive generic algorithm will be incorporated in future work to ensure that the global maximum of the control parameter is obtained.]

Stage one of the optimisation scheme employed begins at transducer No1 (the central transducer), the applied voltage was varied by 25V steps from the minimum to the maximum value (i.e. 0V to 200V). The actuator was then set to the 'best' voltage as determined by the detector i.e. the voltage that maximised the control signal. This procedure was repeated for all 37 actuators in turn and the whole process could be repeated N times. Stage two of the optimisation varied the transducer voltage from –15V to 15V about the previously set 'best' value. Again this was done for all actuators in turn, and repeated M times. For both stages of optimisation all 37 actuator settings were varied only the first pass, on subsequent passes only the middle 19 transducers were adjusted. This modification significantly improves the optimisation speed, and was appropriate since it was found that the outer ring of transducers have only a small effect on the modal properties of the laser.

The time taken for the whole optimisation procedure was variable, however, the results presented below were obtained for N=M=2, and took about 4 minutes to complete. The main limitation in the speed of the optimisation was the graphics capability of the PC used; however the time could be reduced to ~50 seconds using a PC with improved graphics capability. By eliminating the graphics update further speed improvements could be introduced. However, as we are proposing this technique for aberration control of much higher power lasers, the thermal lag of the mode quality as the mirror is transformed will seriously limit the optimisation time.

This optimisation routine gives one solution, which is a local maximum of the control parameter; however the hill-climbing algorithm cannot guarantee that the solution is a global maximum. Stochastic algorithms such as Genetic [10] or Simulated Annealing [11] are required to ensure the global maximum is returned.

5. Determination of the shape of the AO mirror in the laser cavity

Although the shape of the AO mirror can be determined from computer simulations, we examined the actual deformation present as the mirror was operating within the Nd:YVO_4

#1298 - $15.00 US
Received May 30, 2002; Revised June 24, 2002

cavity. A Michelson interferometer was constructed which incorporated the AO mirror as a common element in both the laser cavity and the interferometer. The final configuration, illustrated in figure 5, utilised a HeNe laser operating at 633nm as the illumination source and a CCD camera as a detector. The AO mirror surface was referenced to a λ/20 zerodur mirror, the other 'flatness critical' components were all known to be λ/5 or better over the used aperture.

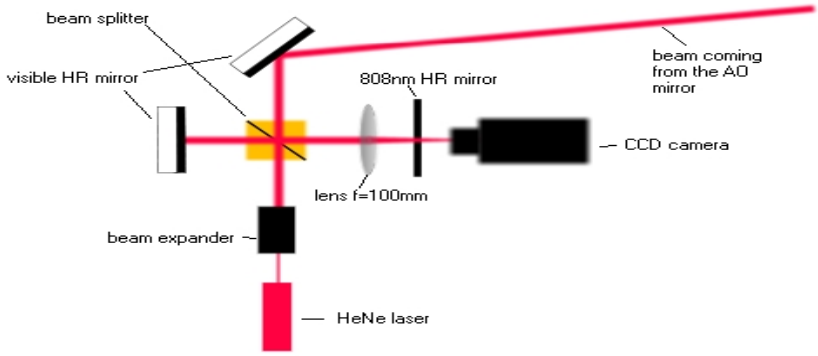

Figure 5. Michelson interferometer arrangement.

6. Results

6.1 Interferometer measurements

With zero bias applied to all 37 actuators, the AO mirror surface was found to be flat to within λ/2 over the entire illuminated aperture (see fig. 6a). On application of known voltages, the interference pattern (see fig. 6b) obtained from theoretical electrostatic calculations were in excellent agreement with the actual shape recorded. Also, it was evident that on blocking the Nd:YVO_4 laser, the fringe pattern of the AO mirror did not alter, indicating that negligible changes in the mirror occurred due to the circulating power within the laser cavity. The AO mirror surface was also monitored during the optimisation sequence in order to investigate any possible delay between the mirror shape changing and the output laser mode altering. Such a delay may be expected due to the changing thermal load within the laser rod and this would have implications for the software control programming and also for the 'settling time' of the optimisation sequence.

Figure 6. Interference patterns recorded form the Michelson interferometer for (a) all the actuators were set at 0V, and (b) all actuators set to 200V.

6.2 Optimisation of transverse mode profile

The initial optimisation routine was examined with a pump power of 6W incident on the Nd:YVO_4 rod. Before optimisation, the output profile was determined to be TEM_{01}. Using a 100μm pinhole as the mode quality detector the evolution of the output was recorded and is reviewed in figure 7. Similar results were obtained using the CCD-based optimisation routine.

#1298 - $15.00 US
Received May 30, 2002; Revised June 24, 2002

Initially the output power from the laser was ~20mW. During the optimisation procedure the transverse mode profile was observed to change substantially, especially when the central transducers were varied. However, as expected the output mode profile converged rapidly towards the desired single-lobed profile after both stage 1 passes were completed. Stage 2 of the optimisation cleaned up the mode distribution further resulting in an accurate TEM_{00} transverse mode profile. Also a consequence of the optimisation: the average output power increased to 120mW. The physical change in the mirror during optimisation is subtle as shown on figure 7. A full interpretation of the interference pattern is beyond the scope of the current paper and is the subject of further investigation.
A real time video of the optimisation procedure is displayed in figure 8.

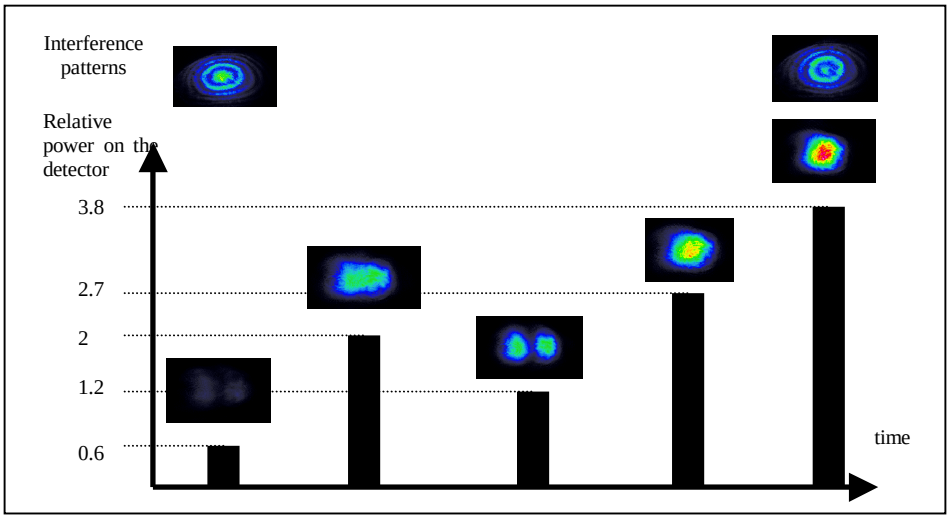

Figure 7. Beam profiles from the Nd:YVO_4 laser and associated interference patterns recorded at various intervals during an optimisation sequence. A histogram of the detected average output power is also shown

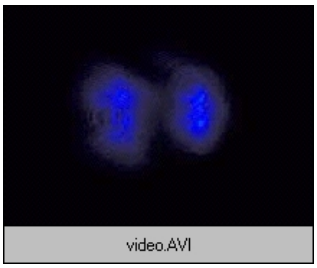

Figure 8. (2.9MB) video of a real time optimisation procedure

7. Conclusion

We have demonstrated automatic spatial mode control by using an electronically addressable 37-element deformable membrane mirror in an all-solid-state laser cavity. Two methods of optimisation have been demonstrated based on a physical aperture arrangement and also a more flexible video based variant. During the optimisation sequence a thermally induced lag was observed, which has consequences on the speed of optimisation specifically during the phase where a large mirror deviation is required. In order to simplify and hence maximise the flexibility of the system, an additional piezo controlled 'tilt' mirror and motorized cavity length control will be required and these improvements are currently under investigation. Using a Michelson interferometer for in-situ determination of the shape of the mirror has proved a reliable method of accurately determining the detailed shape of the AO mirror, and as such reflects the nature of the actual thermal lens induced within the laser rod.

#1298 - $15.00 US
Received May 30, 2002; Revised June 24, 2002